Towards a more Accurate Infrared Distance Sensor Model

Paulo Malheiros, José Gonçalves and Paulo Costa

INESC Porto - Manufacturing Systems Engineering Unit

Faculty of Engineering of the University of Porto

Porto, Portugal

Email: paulo.malheiros@fe.up.pt, goncalves@ibp.pt, paco@fe.up.pt

Abstract

This paper presents the stochastic modelling of an infrared distance sensor. The modelled features of the sensor were its characteristic, the mandatory minimal distance, the sensor noise and the influence of the sensor position while facing an obstacle. In order to model the distance sensor it was necessary to collect a considerable amount of data, for this task it was used an industrial robot to position the distance sensor while facing an obstacle. The presented study is about a Sharp infrared (IR) distance sensor (model GP2Y0A21YK0F).

Introduction

The Sharp family of infrared range finders is very popular for projects that require cheap and somewhat accurate distance measurements. Some drawback of these sensors is their non-linear response and its mandatory minimum distance measurement requisites. Their inherently fast response is attractive for enhancing the real-time response of a mobile robot [1]. Some IR sensors are based on the measurement of the phase shift, and offer medium resolution from 5 cm to 10 m [2], but these are very expensive.

This IR sensor is more economical than sonar rangefinders, yet it provides much better performance than other IR alternatives. Interfacing to most microcontrollers is straightforward: the single analog output can be connected to an analog-to-digital converter for taking distance measurements, or the output can be connected to a comparator for threshold detection. The detection range, suggested by the manufacturer, of this version is approximately 10 cm to 80 cm [3][4], but it offers other models with different measuring ranges. The tested IR sensor (GP2Y0A21YK0F) uses a 3-pin JST connector, when looking at the back, the three connections from left to right are power, ground, and the output signal.

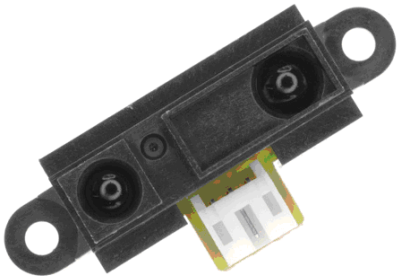

Fig. 1 Sharp infrared sensor.

In order to model the distance sensor it was necessary to collect a considerable amount of data, for this task it was used an industrial robot to position the distance sensor while facing an obstacle. This setup allows the increase of speed and repeatability in the distance sensor data collecting while reducing errors [5][6][7]. The used experimental setup is shown in Figure 2. The industrial robot is the HP6 from Motoman with the NX100 controller available at the Laboratory of Control and Robotics of the Faculty of Engineering of the University of Porto. The robot controller provides a remote mode with its communication based in the protocol described in [8], which uses a standard TCP/IP connection.

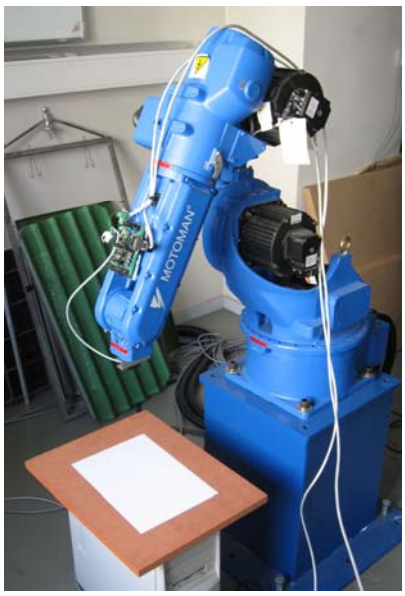

Fig. 2 Experimental setup using Motoman industrial robot.

An interface board with an ATmega8 microcontroller was used to acquire the output voltage from the sensor, sending that information to be stored in a computer. A low-pass filter in the sensor output allows a cleaner measure, having a time constant of 1ms which is considerably lower than the sensors response time of 38 ms [3]. In Figure 3 is a representation of the used electronic circuit.

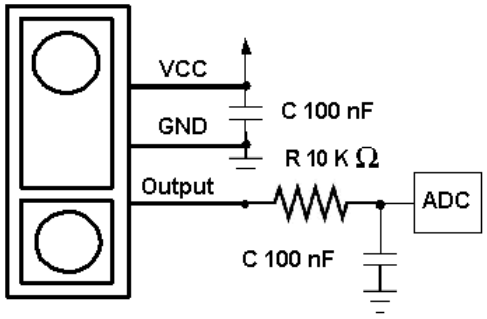

Fig. 3 Sensor electronic conditioning circuit.

A custom-developed software positions the industrial robot and records the sensor output for later processing.

Section 2 introduces the obtained sensor characteristic and its stochastic modelling. Section 3 explains how the sensor should be attached to a robot having in mind the minimal distance and the sensor positioning while facing an obstacle, it also describes the dependability of the sensor measures while facing obstacles with different angles. Section 4 shows the sensor beam and how its shape influences measures especially while facing an obstacle and when there are transitions between obstacles. Finally some conclusions and future work are presented.

Sensor Measuring Characteristics

To determine the stochastic model the sensor was moved in a right angle towards the target from a distance of 80 cm, with intervals of 5 mm in which 128 output samples were acquired.

Initially it was thought that the electromagnetic field generated by the industrial robot actuators could interfere with the sensor measures. In order to quantify this possible interference two test runs were made. On the first run the motors were always on while on the second run the motors were turned off during each acquisition sequence, these are shown in Figure 4.

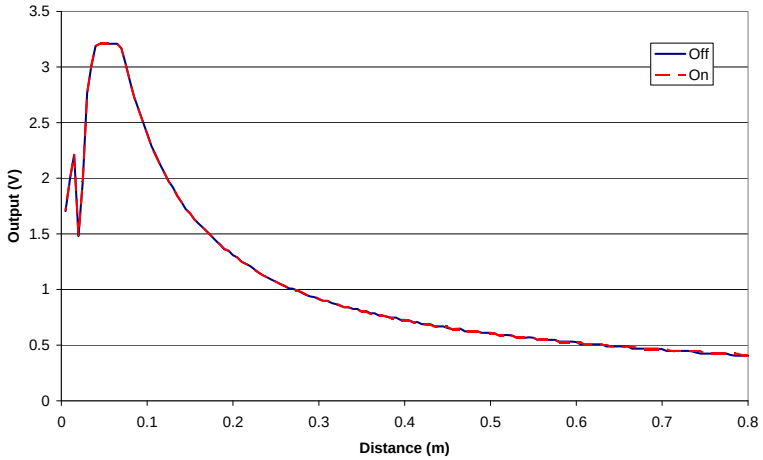

Fig. 4 Output voltage vs. distance curve.

It can be seen that the robots presence is not interfering with the sensor, its output presents a good immunity to electromagnetic noise. One can also attest the sensor repeatability by the superposition of both series (On and Off). The following tests were done with the electric motors always active during the acquisition sequence to speed up the data collecting.

The sensors output is highly non-linear presenting its higher sensitivity in distances between 8 cm and 30 cm, for longer distances the output sensitivity is considerably smaller. Although the manufacturer recommends the use of this sensor for distances bigger than 10 cm, this sensor measures correctly distances from 8 cm, as show in Figure 4. Once the measurement falls below 8 cm the voltage output drops rapidly and appears to be a longer range reading, this phenomenon can be disastrous in sensor applications. For example, in mobile robotics the solution to this problem is to not put your sensor near the front of the robot, but to instead push the sensor into the robot, as shown in Figure 5, so that the border of the robot is located before the minimum sensor range [4].

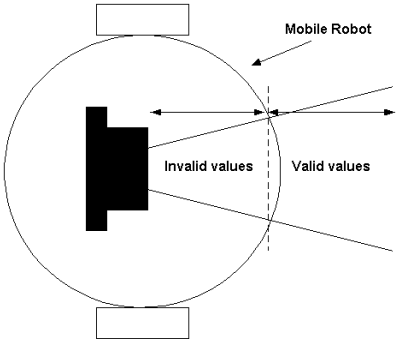

Fig. 5 Sharp sensor location to avoid range errors.

An important sensor property to be modelled is its output voltage noise standard deviation, which helps to define the distance noise.

For this sensor the voltage noise remains almost constant in the working range as shown in Figure 6. For each of the acquisition steps, the standard deviation was determined for all 128 samples.

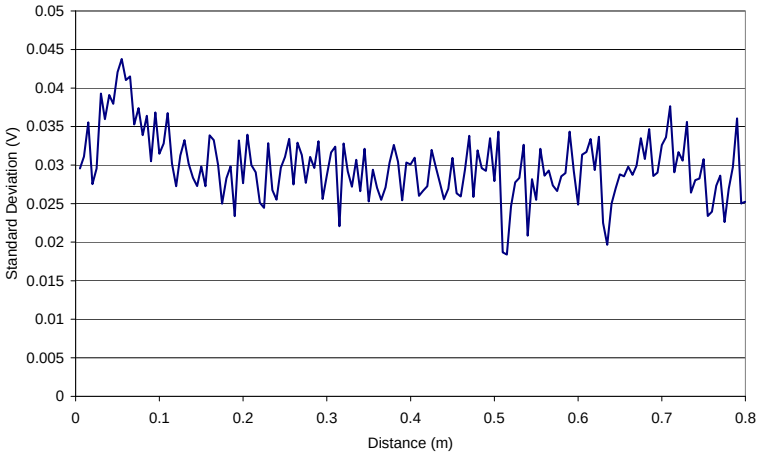

Fig. 6 Sensor output noise to distance curve.

Considering the working range from 8 cm to 80 cm, a linear regression of this noise gives the relation between the output standard deviation (σ_{Output}) to the distance from the target (d), this is approximately a fixed 0.030 mV.

$$\sigma_{Output} = -0.00272d + 0.0304$$

According to the information provided by the manufacturer in a sensor application note [3], the voltage inverse can be approximated to a straight line in the

working range. Figure 7 shows the inverse voltage in function its distance with the respective linear regression.

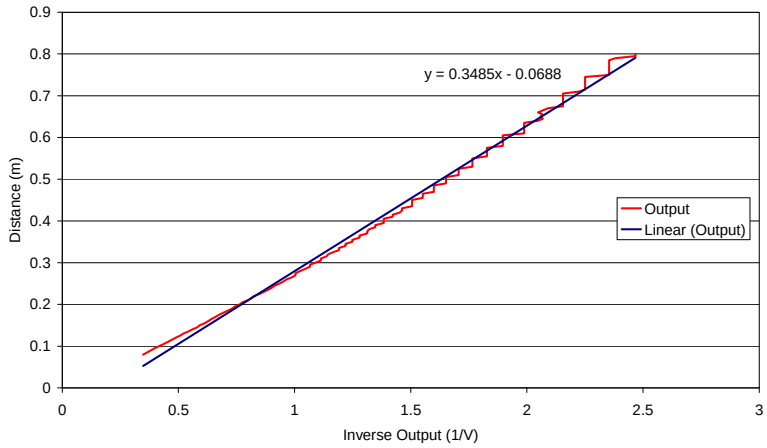

Fig. 7 Distance to inverse voltage output curve and linear regression.

The corresponding linear regression is:

$$d = 0.348\left(\frac{1}{v}\right) - 0.0688$$

This approximation has a total sum of squared error of 0.025 m^2. Despite the low error presented by the model suggested by the manufacturer, a more accurate model can also be obtained using a second-order regression, presented in Figure 8, with its total sum of squared error of 0.0066 m^2.

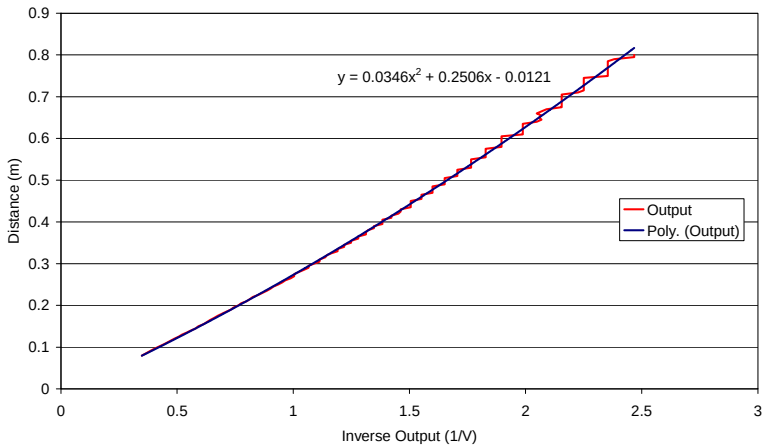

Fig. 8 Distance to inverse voltage output curve and second-order regression.

The new corresponding function is:

$$d = k_1\left(\frac{1}{v}\right)^2 + k_2\left(\frac{1}{v}\right) + k_3$$

In which k_1 has a value of 0.0346, k_2 has the value 0.251 and k_3 the value -0.0121. This function allows determining the distance measure from the output voltage. Its inverse is:

$$v = \frac{-k_2 - \sqrt{4k_1 d + k_2^{\,2} - 4k_1 k_3}}{2(-d + k_3)}$$

In order to obtain the distance variance it was made the approximation shown in Equation 1, with a different derivative for each voltage, where m is the distance derivative presented in Equation 2.

$$d = m.v + b \tag{1}$$

$$m = -\frac{2k_1}{v^3} - \frac{k_2}{v^2} \tag{2}$$

This approximation was made to obtain the distance variance related with the voltage variance.

$$\mathrm{var}(d) = m^2 \, \mathrm{var}(v) \tag{3}$$

Resorting to Equation 3 the graphic presented in Figure 9 is obtained, where it can be observed that the measured distance variance increases with the distance, due to a loss of sensitivity in the sensor output voltage.

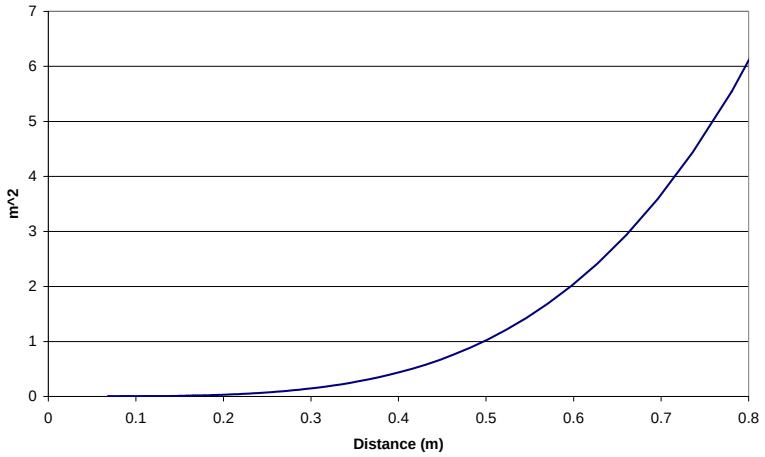

Fig. 9 Distance to variance to distance curve.

Infrared sensors have non-linear characteristics and they depend on the reflectance properties of the object surfaces. So knowledge of the surface properties must be known. In other words, the nature in which a surface scatters, reflects, and absorbs infrared energy is needed to interpret the sensor output as distance measure [9]. To determine the sensors behaviour with different coloured targets two paper sheets were used, one white and the other black, shown in Figure 10. The previous shown tests used the white target.

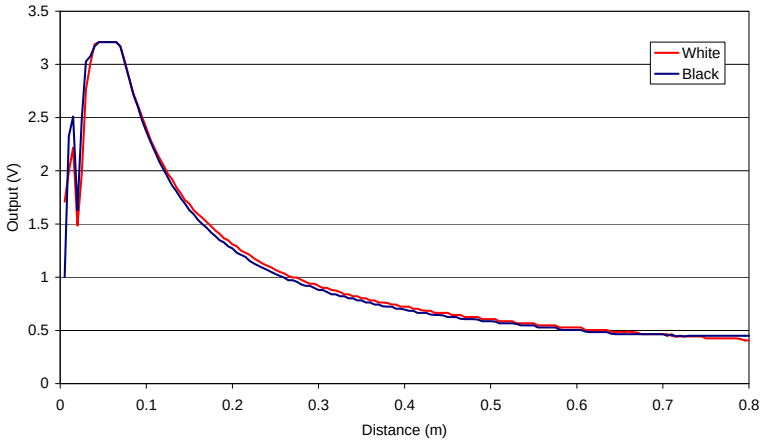

Fig. 10 Output voltage to distance curve for two different targets.

As shown in Figure 10, the output varies with the target colour, although these changes are small. A darker target slightly deviates from the brighter target. A simulated model of this sensor should take into account the colour of the measured target for extra precision. More tests should be done with other target colours and surfaces.

Sensor performance while facing obstacles with different angles

This sensor usability depends largely on its ability to work adequately with non-perpendicular targets. The previous tests were all made with sensor in a right angle with its target.

In order to decrease measuring error by moving direction of obstacle, it is recommend by the manufacturer to mount the sensor as shown in Figure 11.

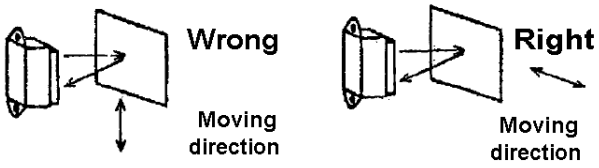

Fig. 11 “Right” vs. “wrong” sensor positioning.

The sensor position is also important in measuring the distance when the obstacle is not in a right angle with the sensor. In Figure 12 is shown the measurement of the sensor in a fixed distance (30 cm) while varying the angle, it is observed that there is a bigger insensitivity in the measure for the “right” position.

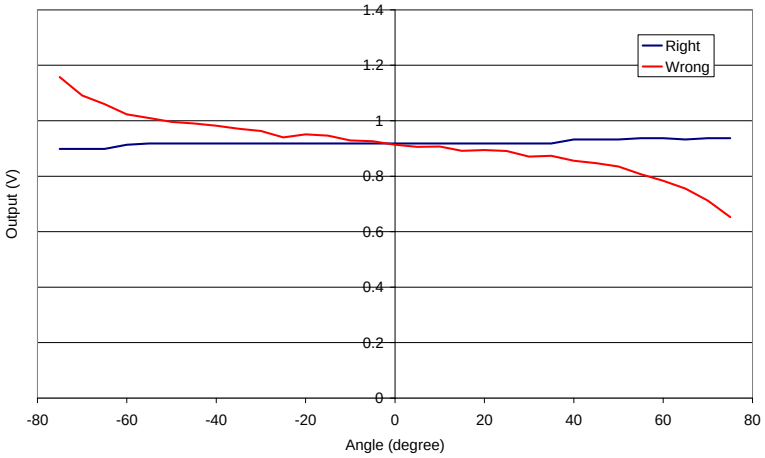

Fig. 12 Sensor performance using the "wrong" and "right" position.

As a consequence, the "right" position of the sensor provides a distance with a great insensitivity in the measure for all the working range of 8 cm to 80 cm. To demonstrate the previous statement the experimental setup shown in Figure 13 was implemented, obtaining the graphics shown in Figure 15 and Figure 16, where it is observed that there is a great insensitivity to the angle variation (up until 75º) mainly from distances of 10 cm to 50 cm. For longer distances the angle effect is visible in the output for smaller angles between sensor and the target.

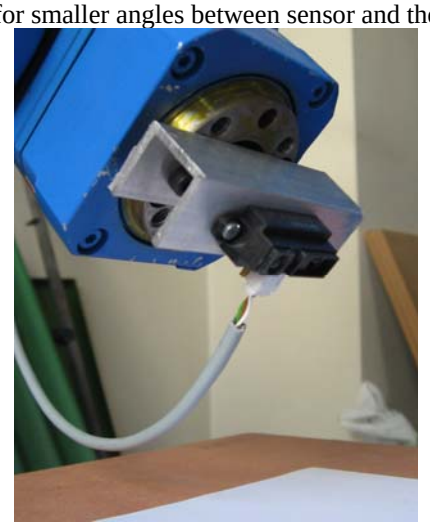

Fig. 13 Sensor positioned in a 45º angle to the obstacle.

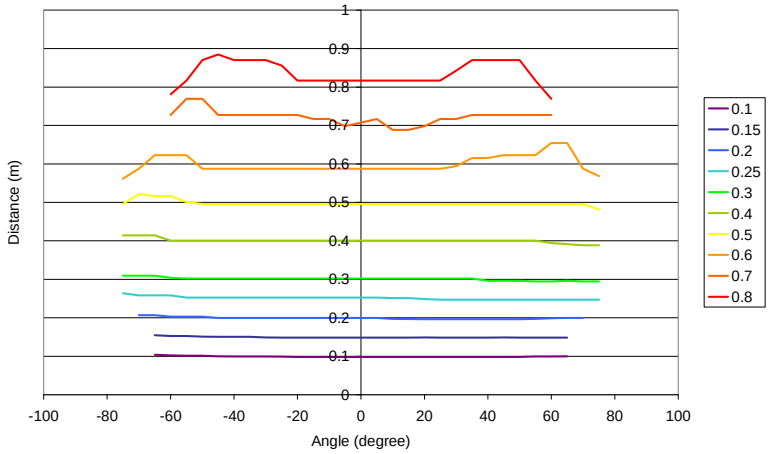

Fig. 14 Sensor performance for a wide range of angles using several fixed distances.

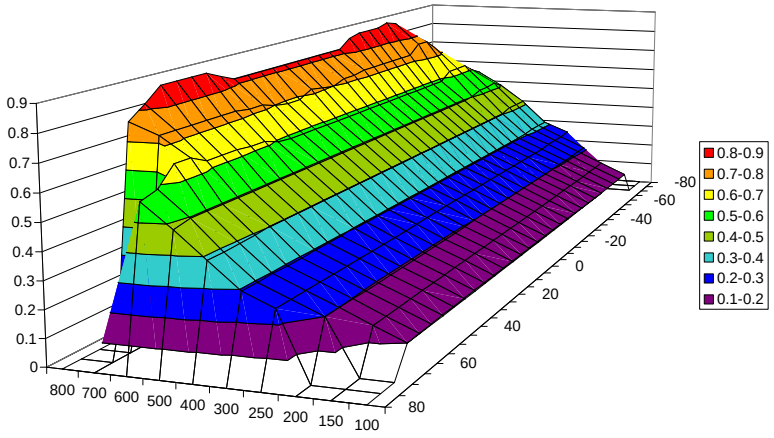

Fig. 15 Measuring area for a wide range of angles.

Beam Pattern Modelling

The infrared beam has some divergence which consists in an angular measure of the increase in beam diameter with distance from the optical aperture. This phenomenon should be taken into account while modelling this sensor. The use of an infrared sensitive camera allowed estimating the beam diameter for different distances, through image processing, as shown in Figure 16.

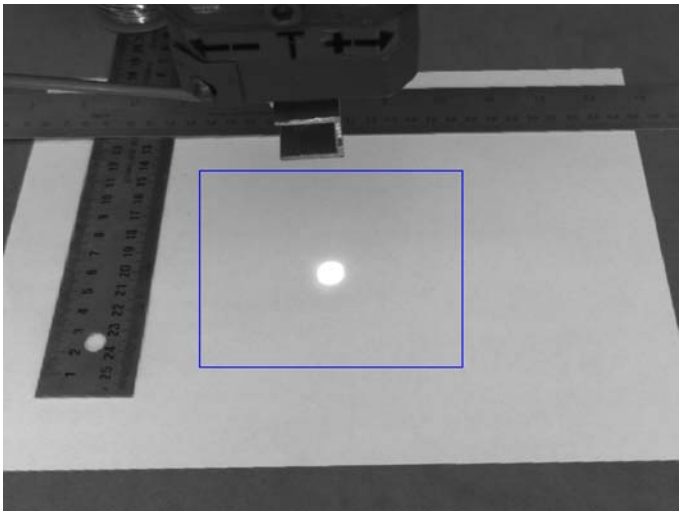

Fig. 16 Beam projection in obstacle. Area of analysis highlighted.

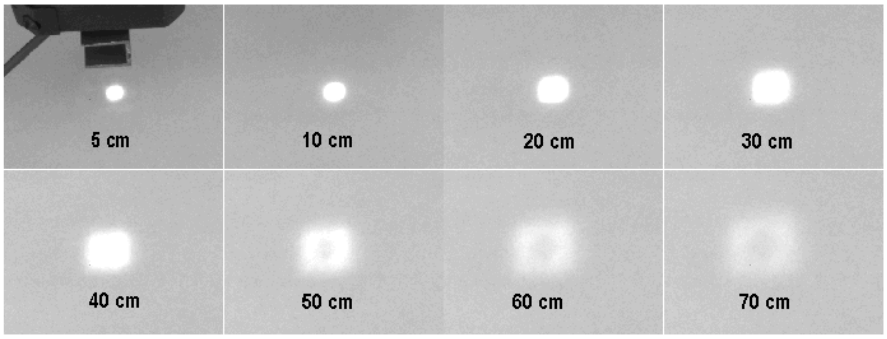

Fig. 17 Beam projection sequence using different obstacle distances.

The measured beam diameter, shown in Figure 17, grows somewhat linearly with the distance. Hence this beam can be approximated to a cone shape.

This can be modelled through the linear regression described by Equation 4.

$$\varnothing = 0.0399d + 0.0083 \tag{4}$$

Therefore the linear regression slope is the beam divergence of 0.0399.

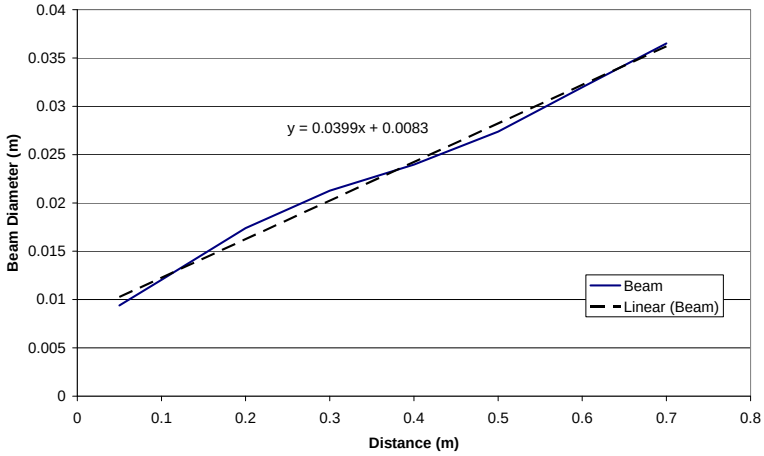

Fig. 18 Beam diameter to distance curve.

One can also visually analyse the beam behaviour with the increase of the angle. The sequence, shown in Figure 19, shows the image of the beam with different angles from a fixed distance of 20 cm. It can be seen that up until a 70º angle the beam pattern appears well focused on the target, while at 80º the beam is very disperse. This demonstrates how the sensor is able to measure with great immunity for different angles while facing an obstacle, as discussed in the previous section.

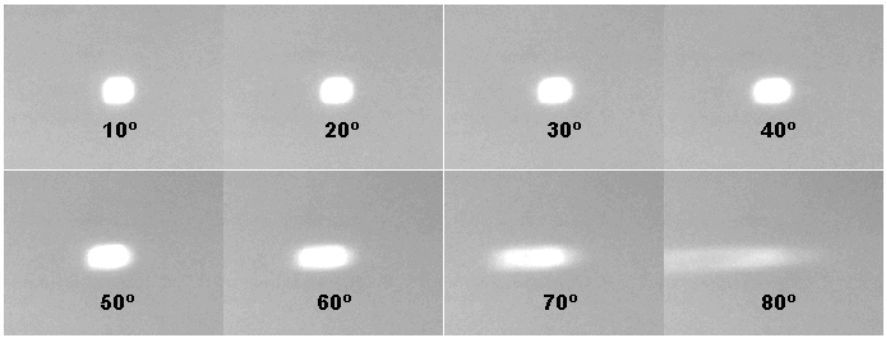

Fig. 19 Beam projection sequence using different angles to obstacle.

It is necessary to take into account that when measuring longer distances the beam spreads over a larger area, forcing a higher error during transitions between planes, in Figure 20 is represented the executed test. In Figure 21 and Figure 22 are shown the measure between two planes which are 10 cm apart. As expected for a longer distance it has a wider transition range in order to obtain a correct measure.

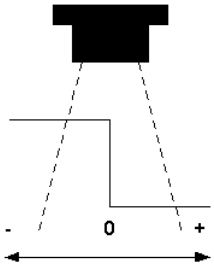

Fig. 20 Transition test for IR sensor.

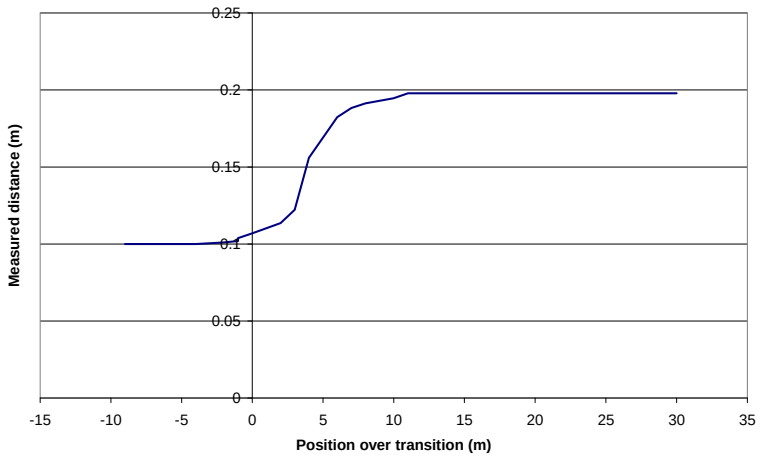

Fig. 21 Measured distance progression through a 10 cm to 20 cm step.

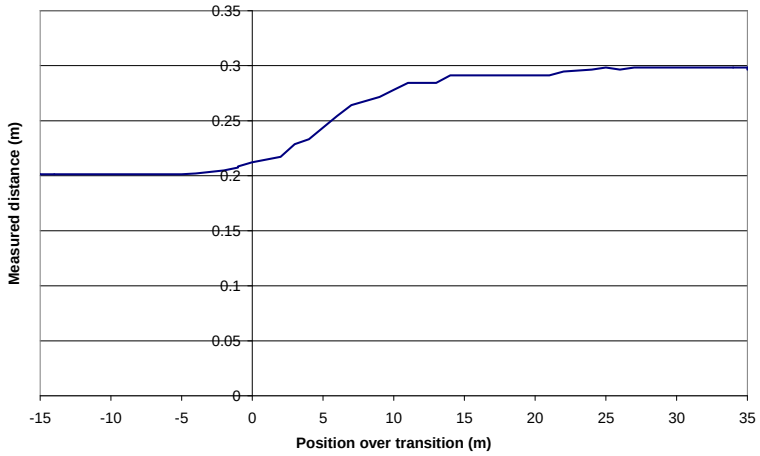

Fig. 22 Measured distance progression through a 20 cm to 30 cm step.

Conclusion and Future Work

This paper presented the stochastic modelling of an infrared distance sensor. The modelled features of the sensor were its characteristic, the mandatory minimal distance, the sensor noise and the influence of the sensor position while facing an obstacle. It is described the sensor interface, both electronic and mechanic, in order to improve the robustness and reliability of the sensor measures. In order to model the distance sensor it was necessary to collect a considerable amount of data, for this task it was used an industrial robot to position the distance sensor while facing an obstacle.

As future work fast moving tests should be performed to model the dynamic properties of this sensor. It is also intended to simulate the sensor in a virtual environment, having in mind all the features that were included in the proposed model.

References

[1] G. Benet, F. Blanes, J.E. Simo, P. Perez, "Using infrared sensors for distance measurement in mobile robots," Journal of Robotics and Autonomous Systems, vol. 10, 2002, pp. 255-266.

[2] T. Mohammad, "Using Ultrasonic and Infrared Sensors for Distance Measurement", World Academy Of Science, Engineering And Technology, Volume 51, March 2009

[3] Sharp GP2Y0A21YK0F Sensor Datasheet

[4] Sharp IR Rangers Info, http://www.acroname.com/robotics/info/articles/sharp/sharp.html, retrieved on October 28, 2009.

[5] M. Groover, M. Weiss, R. Nagel, N. Odrey, "Industrial Robotics: Technology, Programming, and Applications", McGraw-Hill, 1995.

[6] H. Colestock, "Industrial Robotics: Selection, design and maintenance", McGraw-Hill, 2005.

[7] José Gonçalves, José Lima, Hélder Oliveira and Paulo Costa, "Sensor and actuator modeling of a realistic wheeled mobile robot simulator", 13th IEEE International Conference on Emerging Technologies and Factory Automation Hamburg, 15-09-2008

[8] Yaskawa Electric Corporation (Japan), "NX 100 applications options -Instructions for data transmission function", August 2004.

[9] P.M Novotny, N.J. Ferrier, "Using infrared sensor and the Phong illumination model to measure distances," International Conference on Robotics and Automation, Detroit, MI, vol. 2, April 1999, pp. 1644- 1649.